



HAL
open science

Comparison of Blind Source Separation Methods to Surface Electromyogram for Extensor Muscles of the Index and Little Fingers

Abilé Magbonde, Franck Quaine, Bertrand Rivet

► **To cite this version:**

Abilé Magbonde, Franck Quaine, Bertrand Rivet. Comparison of Blind Source Separation Methods to Surface Electromyogram for Extensor Muscles of the Index and Little Fingers. EMBC 2022 - 44th Annual International Conference of the IEEE Engineering in Medicine & Biology Society, Jul 2022, Glasgow, United Kingdom. pp.3615-3618, 10.1109/EMBC48229.2022.9870902 . hal-03961323

HAL Id: hal-03961323

<https://hal.science/hal-03961323>

Submitted on 28 Jan 2023

HAL is a multi-disciplinary open access archive for the deposit and dissemination of scientific research documents, whether they are published or not. The documents may come from teaching and research institutions in France or abroad, or from public or private research centers.

L'archive ouverte pluridisciplinaire **HAL**, est destinée au dépôt et à la diffusion de documents scientifiques de niveau recherche, publiés ou non, émanant des établissements d'enseignement et de recherche français ou étrangers, des laboratoires publics ou privés.

Comparison of Blind Source Separation Methods to Surface Electromyogram for Extensor Muscles of the Index and Little Fingers

Abilé Magbonde, Franck Quaine and Bertrand Rivet

Abstract—Crosstalk is the result of the propagation of muscle electrical signals on surface electromyogram channels simultaneously. The objective of this paper is to study the behavior of three blind source separation (BSS) methods for crosstalk reduction during finger extensor muscle contractions: FastICA, joint diagonalization of covariance matrices and optimal filtering. These methods have been tested on artificial mixtures defined by a temporal sum of the real signals from isolated contraction of two independent biomechanical muscles for the extension of the index and little finger. Artificial mixtures display a ground truth for comparison between the methods. The separation was better using the optimal filtering compared to the other two methods. The optimal filtering have then be tested on real mixtures recorded during a simultaneous contraction of the two muscles. The results are less satisfactory but open doors to new perspectives.

I. INTRODUCTION

Electromyogram (EMG) relates to the muscular activity of the muscular fibers when a muscle is in contraction. It is widely used in biomechanical studies and in medicine [1], e.g., for the production of prostheses control or the rehabilitation of the hand. In this study, we seek to extract the activity of the extensor muscles of the index and little fingers in a non-invasive way using the surface electromyogram (sEMG) by placing electrode matrices on the surface of the skin. Since these narrow muscles are close to each other, the sEMG is affected by crosstalk [2], [3] when the two fingers are in simultaneous contraction. One way to extract activity for each muscle from the sEMG recordings can be to apply blind source separation (BSS) methods [4], which aims at recovering individual sources from mixtures of them. In this article different BSS methods based on different assumptions are compared when applied on the sEMG for extensor muscles of index and little finger.

The article is divided as follows. Section 2 introduced the separation methods used. Section 3 presents the experimental protocol before numerical results in Section 4 and discussion and conclusions in Section 5.

II. METHODS

For the comparison, three methods (FastICA [4], joint diagonalization of covariance matrices [5] and optimal filtering [6]) have been selected according to the specificity of the sEMG. Indeed, a classical modeling of the sEMG is a linear instantaneous mixture of the activation potentials

generate by each muscle fiber, leading to

$$\mathbf{x}(t) = \mathbf{A}\mathbf{s}(t) + \mathbf{n}(t), \quad (1)$$

where $\mathbf{x}(t) \in \mathbb{R}^P$ is the vectors of P signals recorded by each sensor, $\mathbf{s}(t) \in \mathbb{R}^N$ is the vector of N sources representing the muscle fibers and $\mathbf{A} \in \mathbb{R}^{P \times N}$ is the mixing matrix and $\mathbf{n}(t) \in \mathbb{R}^P$ is the additive noise gathering all the remaining activities such as artefacts or electronic noise.

A. FastICA method

As the first selected method, FastICA [4] is a generic BSS method which only assumes that the sources $\mathbf{s}(t)$ in (1), considered as stochastic processes, are mutually independent. FastICA aims at estimating a demixing matrix $\mathbf{W} \in \mathbb{R}^{P \times P}$ so that the estimated components

$$\mathbf{y}(t) = \mathbf{W}\mathbf{x}(t) \quad (2)$$

are as mutually independent as possible, measured by the mutual information between them using high order statistics based on the fact that the different sources are thus not normally distributed.

Applied on sEMG, the underlying assumption is that the activities of different muscles are independent to each other, meaning that the considered muscles are biomechanically independent. Nevertheless, each muscle is composed of a large number of muscle fibers each of them being thus considered as a source, $s_i(t)$. These later are not mutually independent if they belong to the same muscle.

B. Joint diagonalization of covariance matrices

The joint diagonalization of covariance matrices [5] also belongs to the independent component analysis family. As FastICA, it aims at estimating a demixing matrix \mathbf{W} so that the estimated sources (2) are as independent as possible. Unlike FastICA, this method only use second order statistics based on the assumption that the sources are non-stationary. Especially, this method assumes that the power of the sources is time-varying and that these variations are not the same for the different sources. Several covariance matrices, \mathbf{C}_i , of the recordings $\mathbf{x}(t)$ are computing using a sliding window. The set $\{\mathbf{C}_i\}_i$ of these matrices is then joint-diagonalized by a single demixing matrix \mathbf{W} so that

$$\forall i, \quad \mathbf{W}\mathbf{C}_i\mathbf{W}^T = \Lambda_i, \quad (3)$$

where Λ_i is a diagonal matrix.

The assumption of this method is quite accurate for sEMG as long as the intensities of the muscles involved in a movement do not evolve in the same way (up to a scaling factor).

C. Optimal filtering

Optimal filtering [6] is a semi-blind source separation method in the sense that it requires a reference signal corresponding to the recording of the sEMG when only the target muscle is in contraction in addition to the recordings when several muscles are involved simultaneously. Let $\mathbf{x}_1(t)$ denote the sEMG when only the target muscle is in contraction and $\mathbf{x}_2(t)$ the sEMG when several muscles are in contraction simultaneously. The optimal filtering aims at estimating a demixing matrix \mathbf{W} so that the estimated sources (2) maximize the signal to signal-plus-noise ratio (SSNR) defined as

$$SSNR(\mathbf{W}) = \frac{\mathbf{W} \boldsymbol{\Sigma}_1 \mathbf{W}^T}{\mathbf{W} \boldsymbol{\Sigma}_2 \mathbf{W}^T}, \quad (4)$$

where $\boldsymbol{\Sigma}_1$ (resp. $\boldsymbol{\Sigma}_2$) is the covariance matrix of $\mathbf{s}_1(t)$ (resp. $\mathbf{s}_2(t)$). This method is quite similar to the joint diagonalization method (Section II-B) since it is based on joint diagonalization of only two covariance matrices. The main difference is that the optimal filtering requires that one of the two matrices is related to a time window during which only the target muscle is in contraction. Moreover, the estimated components with the highest SSNR are related to the target muscles but the components with the lowest SSNR remain mixtures of the other muscles. It is also worth noting that this method needs a calibration in the sense that the sEMG must be recorded when the target muscle is in contraction alone to compute $\boldsymbol{\Sigma}_1$ in (4). This later requirement can be a major drawback if the studied muscles are not biomechanically independent.

III. EXPERIMENTAL PROTOCOL

The protocol was based on the Extensor Digitorum Communis (EDC) muscle analysis for the index and the little fingers (EDC_I and EDC_L). These muscles are in a close area and are biomechanically independent [7], meaning it is possible to isolate their respective involvement during specific task requirements [8]. In the current paper, EDC_I and EDC_L sEMG signals are acquired during extension movements in given sequences.

A. Subjects

EMG signals were recorded on 10 healthy subjects including 08 men and 02 women volunteers who signed a consent form. These subjects are in good health and do not present pathologies in the forearm. The average age is (28.5 ± 11.7) years.

B. sEMG acquisition

The signals were recorded using an 8x8 size matrix with an interelectrode distance of 10mm. The array was placed on the forearm (Fig. 1.) following the instructions in [9]. The skin had to be prepared by shaving it and then applying the abrasive paste. The signals were amplified with the Quattrocento (OT Bioelectronica, Torino, Italy) acquired in monopolar mode at a frequency of 2048 Hz, digitally

converted (16 bit A/D converter) and bandpass filtered 10-500 Hz. Two reference electrodes were placed on the distal part of the ulna and radius, next to the wrist joint.

Each subject performed 10 extension movements with a maximum amplitude for different finger tasks. Three tasks were performed: 15s individual index extensions for EDC_I , 15s individual little extensions for EDC_L , and simultaneous 30s finger extensions for both EDC_I or EDC_L . For simultaneous extensions, the task began with 5s rest, then 15s of contraction of EDC_I (versus EDC_L) followed by 15s contraction of EDC_L (versus EDC_I) with 10s overlapping. The recording stopped after 5s rest at the end.



Fig. 1. The 64-channel electrode grid (8x8 channels, 10 mm inter-electrode-distance) used to record the sEMG activity from extensors of index and little finger

C. Artificial Signal

Artificial sEMG signals were obtained from the real signals gathered from the individual contraction of EDC_I and EDC_L . The different artificial mixtures are made by a temporal sum of the signals of muscles of both fingers Fig. 2).

For each subject, 30 mixtures are obtained by summing the index and little finger signals randomly selected from the 10 extension movements recorded separately.

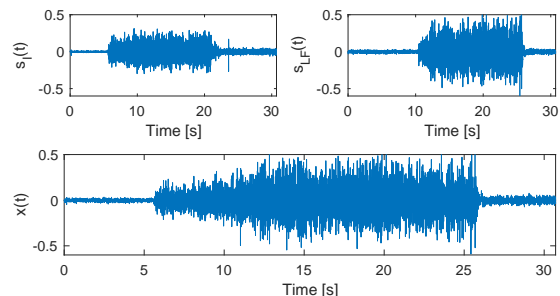


Fig. 2. Artificial mixture of one electrode on the 64. Top left (res. right): signal $s_I(t)$ (resp. $s_{LF}(t)$) corresponds to the extension of the index (resp. little finger) alone. Bottom: artificial mixture $x(t) = s_I(t) + s_{LF}(t)$.

D. Choice of components

By applying each method on artificial mixtures, since we have $P = 64$ sensors, we estimate 64 components (*i.e.* $\mathbf{y}(t) \in \mathbb{R}^{64}$). However, only a subset belong to the signal subspace and the others to the noise subspace. We are obviously interested in the first type of component that we will have to select.

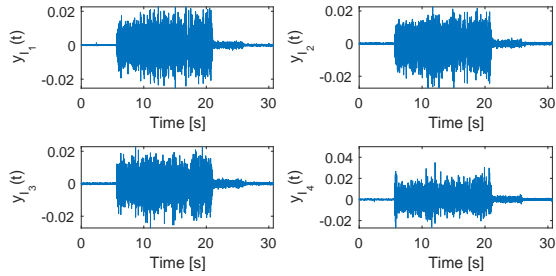


Fig. 3. Four components $y_{I_k}(t), k \in \{1, \dots, 4\}$, of the index that maximizes the signal to signal-plus-noise ratio (SSNR) out of the 64 estimates provided by the optimal filtering.

The interest of the artificial mixture is that we know its composition precisely. As a result, from the power profile of the target source that we would like to estimate, we are able to choose the different estimated components. A comparison is then made between the power profiles of the target with those of the 64 components, leading to select those related to the target signal. Let $\mathbf{y}_I(t) \in \mathbb{R}^{N_I}$ and $\mathbf{y}_{LF}(t) \in \mathbb{R}^{N_{LF}}$ refer to the selected components when the index (N_I) and the little finger (N_{LF}) are the target muscles, respectively. Figure 3 shows 4 components selected after estimation by optimal filtering applied on mixture presented Fig. 2 when trying to extract activity related to index.

IV. RESULTS

In this section, the criteria used to numerically evaluate the performance of the extraction methods are described before the numerical results obtained on the data.

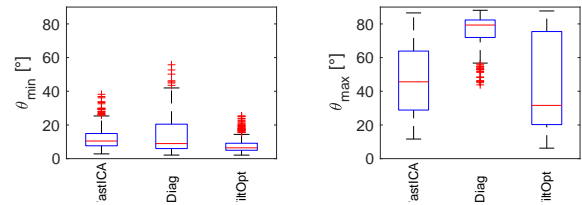
A. Metrics of evaluation

Classically to evaluate the performance of source separation methods, one can refer to the widely used criteria such as signal to interference ratio or signal to distortion ratio [10]. However, they cannot be used on actual data such as sEMG since they depend on the true sources $s_i(t)$ which remain unknown on actual sEMG (it would require to record the electrical activity of all muscle fibers which is impossible).

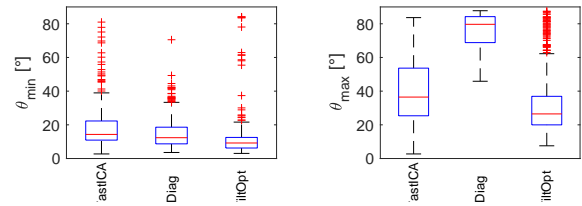
To overcome this difficulty, we propose two numerical criteria to quantify the performance of separation based on the fact that in our experiment we have access to the sEMG when single finger was in contraction (Section III). These signals are denoted $\mathbf{z}_I(t) \in \mathbb{R}^P$ and $\mathbf{z}_{LF}(t) \in \mathbb{R}^P$ when respectively the index and the little finger are in contraction alone. Thus, the quality of separation is defined as the minimal θ_{min} and maximal θ_{max} principal angles [11] between the subspace spanned by the selected components $\mathbf{y}_{target}(t)$ and the subspace spanned by the reference signals $\mathbf{z}_{target}(t)$, $target$ refers to I (resp. LF) if the index (resp. the little finger) is the target muscle

$$\theta_{min} = \min_k \text{acos}(\sigma_k) \quad (5a)$$

$$\theta_{max} = \max_k \text{acos}(\sigma_k) \quad (5b)$$



(a) Little finger (EDC_L)



(b) Index (EDC_I)

Fig. 4. Performance of separation to extract the little finger (Fig. 4(a)) and index (Fig. 4(b)). In each figure, the minimum (left) and maximum (right) angles are presented for each method. Each box plot shows the median as central red line, the bottom and top edges are the 25th and 75th percentiles, respectively. The whiskers extend to extreme values and the outliers are plotted as red crosses.

with $\{\sigma_k\}_k$ are the singular values of $\mathbf{Q}_y^T \mathbf{Q}_z$, where \mathbf{Q}_y (resp. \mathbf{Q}_z) defines an orthonormal base of the subspace spanned by the selected components $\mathbf{y}_{target}(t)$ (resp. the reference signals $\mathbf{z}_{target}(t)$).

These two metrics are such that $0 \leq \theta_{min} \leq \theta_{max} \leq 90^\circ$, and measure the closeness between the estimated components and the reference signals. Indeed, an angle of 0° means that the estimated components lies in the subspace spanned by the reference signals while an angle of 90° means that the estimated components are uncorrelated with the reference signals. Consequently, θ_{min} (resp. θ_{max}) refers to the best (resp. worst) estimated components: the closer to 0, the better.

B. Numerical results on artificial mixtures of actual data

The three methods of extracting the target muscle, referred to as ‘FastICA’ for FastICA (Sec. II-A), ‘JDiag’ for the joint diagonalization of covariance matrices (Sec. II-B) and ‘FiltOpt’ for the optimal filtering (Sec. II-C), respectively, are applied on artificial mixtures of actual sEMG as described in Section III-C. 30 random mixtures of little finger and index signals are created for each subject, leading thus to 270 artificial mixtures for each target muscle.

Figure 4 shows the quality of separation to extract the little finger (Fig. 4(a)) or the index (Fig. 4(b)). As one can see from the best estimation (θ_{min}), for both index and little finger as target muscle, the methods are ranked as FiltOpt $<$ JDiag $<$ FastICA when looking at the median values, where $A < B$ means that A is better than B . It is also worth noting that the consistency of the methods, measured by their dispersion of performance (*i.e.* distance between the 25th and 75th percentiles), ranks the methods as FiltOpt $<$ FastICA $<$ JDiag. As expected, FiltOpt leads to the best results but it

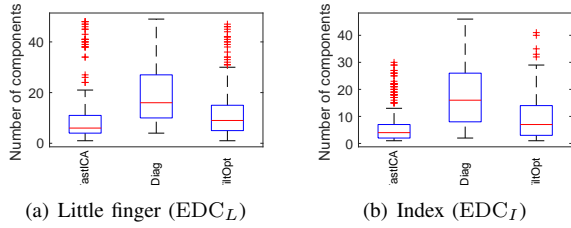


Fig. 5. Number of selected components. Fig. 5(a): the little finger is the target muscle. Fig. 5(b): the index is the target muscle. Each box plot shows the median as central red line, the bottom and top edges are the 25th and 75th percentiles, respectively. The whiskers extend to extreme values and the outliers are plotted as red crosses.

requires a calibration as detailed in Sec. II-C, while FastICA and JDiag are fully blind methods.

When looking at θ_{max} the optimal filtering still leads to the best values. The larger values for JDiag compared to FastICA can be explained by the number of components selected by the different methods (Figure. 5). Indeed, as one can see, the number of selected components is larger for JDiag than for FastICA reflecting a better selectivity of the latter method. As a consequence, it leads to incorporate more noise than signal by selecting additional components. This aspect can be improved by proposing a better selection of components.

From these results, one can conclude that the optimal filtering is the best choice if a calibration session is possible. On the contrary, the joint diagonalization of covariance matrices should be used but the selection of the most accurate number of components must be improved.

C. Illustration on actual mixtures

In this section, we are interesting in analyzing the performance of the optimal filtering for actual mixtures of several muscles. Indeed, in the original paper [6] presenting the optimal filter for sEMG, only validation on artificial simulated signals are presented.

In this section, the calibration data used to compute Σ_1 (Sec. II-C) is different than the one used in the mixture to compute Σ_2 . As illustrating in Figure 6, the optimal filtering provides slightly disappointed results compared to the artificial mixtures presented in the previous section. Indeed, the power of the best component computed using a sliding window of 100ms does not highlight a clear profile in relation to the experimental protocol: the index (resp. little finger) was in extension between 6s to 16s (resp. 11s to 21s). One can see that the activities related to the index and to the little finger are not well separated. If during the first part, the activity of the index is well estimated, this is clearly not the case during the period when the two fingers are in extension (*i.e.* 11s to 16s).

V. CONCLUSIONS

In this paper, three source separation methods (FastICA [4], joint diagonalization of covariance matrices [5] and optimal filtering [6]) have been compared to estimate

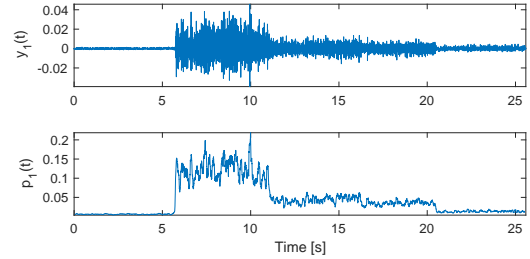


Fig. 6. Illustration of estimated index activity from actual sEMG signal. On top: best estimated component. On bottom: its related instantaneous power.

the activity of extensor digitorum communis muscle for the index and little fingers.

The performance of these separation methods on real sEMG signals but on artificial mixtures has shown that optimal filtering lead to the best estimation, while JDiag is slightly better than FastICA (FiltOpt < JDiag < FastICA). However the optimal filter requires a calibration phase during which the target muscle must be in contraction alone: this can be difficult to achieve in real situation if the involved muscles are not biomechanically independent to each other as the muscles in the leg.

Applied on actual mixtures, the separation of the optimal filtering does not clearly separate the muscles activities. Some preliminary studies would tend to show that could come from some inconsistency of the subspaces related to the two muscles or from their proximity. This will be investigated in future researches.

REFERENCES

- [1] A.D. Roche, H. Rehbaum, D. Farina and O. C. Aszmann. Prosthetic Myoelectric Control Strategies: A Clinical Perspective. *Curr Surg Rep* 2,44, 2014.
- [2] C. J. De Luca and R. Merletti. Surface myoelectric signal crosstalk among muscles of the leg. *Electroencephalogr. Clin. neurophysiol.* 69(6):568–575, 1988.
- [3] D.A. Winter, A. J. Fuglevand, and S.E. Archer. Crosstalk in surface electromyography: theoretical and practical estimates. *J Electromyogr Kinesiol.* 4(1):15–26, 1994.
- [4] P. Comon and C. Jutten. *Handbook of Blind Source Separation: Independent component analysis and applications.* Ac. press, 2010.
- [5] D.-T. Pham and J.-F. Cardoso. Blind separation of instantaneous mixtures of nonstationary sources. *IEEE Trans. Sig. Proc.*, 49(9):1837–1848, 2001.
- [6] L. Mesin. Optimal spatio-temporal filter for the reduction of crosstalk in surface electromyogram. *J. Neural Eng.* 15(1):016013, 2018.
- [7] J. N. Leijnse, N. H. Campbell-Kyureghyan, D. Spektor, and P. M. Quesada. Assessment of individual finger muscle activity in the extensor digitorum communis by surface emg. *J. Neurophysiol.* 100(6):3225–3235, 2008.
- [8] F. Quaine, F. Paquet, F. Letu e, and F. Moutet. Force sharing and neutral line during finger extension tasks. *Hum. Mov Sci.* 31(4):749–757, 2012.
- [9] R. M. Buschbacher. *Anatomical Guide for the Electromyographer: The Limbs and Trunk.* Charles C Thomas Pub Ltd, 2011.
- [10] E. Vincent, R. Gribonval, and C. Fevotte. Performance measurement in blind audio source separation. *IEEE Transactions on Audio, Speech, and Language Processing*, 14(4):1462–1469, 2006.
- [11] G. H. Golub and . F. Van Loan. *Matrix Computation.* Johns Hopkins University Press, third edition, 1996.